Supporting Information

Lithium–Organic Nanocomposite Suspension for High-Energy-Density Redox Flow Batteries

Hongning Chen, Yucun Zhou and Yi-Chun Lu *

Department of Mechanical and Automation Engineering, The Chinese University of Hong Kong, Shatin N.T., Hong Kong SAR, China.

*E-mail: yichunlu@mae.cuhk.edu.hk

Experimental Section

Materials: All chemicals were used as received. Ketjen Black EC-600JD (KB) was received from AzkoNobel. 10-Methylphenothiazine (MPT), lithium hexafluorophosphate ($LiPF_6$), iodine, 1,4-dioxane, ethylene carbonate (EC) and diethyl carbonate (DEC) were received from Sigma-Aldrich. Silver hexafluorophosphate ($AgPF_6$) was received from TCI Chemicals. Carbon paper (HCP010N) was received from Shanghai Hesen Electric Co. Ltd. Lithium foil was received from Shenzhen Meisen Electromechanical Co. Ltd.)

Preparation of MPT-KB Composite: The MPT and KB were mixed to grind homogenously with a mass ratio of 37:1 for 20MPT-5KB and 74:1 for 40MPT-5KB. Then the mixture was transferred to the dry oven and heated at 100 ^{o}C to make the MPT melt with KB for 4 hours. Finally, the recrystallized composite was further grinded for better mixing.

Preparation of LIONS Posolyte: All the suspensions reported herein were made with an electrolyte of 0.3 M MPT in 1 M $LiPF_6$ EC and DEC (volume ratio 1:1). The active materials (MPT or MPT-KB composite) and KB were mixed in a 10 ml glass container with the electrolyte followed by sonication using SLPt Cell Disruptor for 10 min, and then moved to water bath ultrasonication for another 30 min before testing.

Solubility of MPT^+: 10-Methylphenothiazine hexafluorophosphate ($MPTPF_6$) was synthesized as reported by Litt and Summers [Cation Radical Salts of N-Methylphenothiazine and Its Analogs. Synthesis and Characterization. *J. Phys. Chem.* **1974**, 78, 1750-1754.] as follows: 0.0078 mol MPT was dissolved in sufficient ethanol to get an almost saturated solution at about 60° and 0.00385 mol of iodine dissolved in 10 ml of ethanol was added. After a few minutes a solution of 0.0078 mol of silver

hexafluorophosphate ($AgPF_6$) in 5 ml of ethanol was poured in. A precipitate of AgI was formed immediately. The precipitate was filtered off, leaving a red solution of $MPTPF_6$. After evaporation in vacuum at room temperature the salt had the appearance of a black powder. The product was recrystallized by dissolving in acetone (saturated solution) adding 1,4-dioxane (1/3 volume of acetone) and precipitating the crystals out by slow evaporation of acetone under reduced pressure at 80°C.

Assembly of the Static Cell: Figure S9a in the Supporting Information shows the structure of the static cell. One piece of lithium foil (16 mm diameter) was placed onto the bottom stainless steel cell body. One Celgard 2325 separator (18 mm diameter) was placed on the lithium foil. 40 μL electrolyte (1 M $LiPF_6$ in EC and DEC (1:1 v/v)) was added on the separator. One piece of NASICON-type structured $Li_{1.5}Al_{0.5}Ge_{1.5}(PO_4)_3$ (LAGP) ceramic membrane was placed on the Celgard separator. 10 μL MPT posolyte was added on the surface of LAGP with the zero-gap channel. A piece of carbon paper (12 mm diameter) was placed on the posolyte as a current collector followed by 20 μL electrolyte to wet the carbon paper. Finally, a stainless steel spring and a polytetrafluoroethylene (PTFE) O-ring were placed on the cell. Two cell bodies (bottom and top) were separated by a polytetrafluoroethylene spacer to avoid a short circuit. The detailed synthesis process of LAGP can be found in our previous work (Chen et al. *Chem. Mater.* 2017**,** 29). The cell assembly process was conducted in an Ar-filled glove-box (Etelux, <1.0 ppm H_2O and <1.0 ppm O_2).

Assembly of the Flow Cell: Figure S9b in the Supporting Information shows the structure of the flow cell. One piece of lithium foil (2 mm×10 mm) was attached to a stainless steel bottom cell body, which acted as a current collector for the negative electrode. One Celgard 2325 separator (4 mm×14 mm) were placed on the surface of the lithium foil followed by adding 20 μL of electrolyte. One piece of LAGP ceramic membrane (4 mm×12 mm) was placed on the Celgard separator. A Teflon channel

spacer (2 mm thickness) was placed between the bottom cell body and a piece of carbon paper (2 mm×5 mm) was attached to an outer top cell body as a current collector fixed by 6 bolts. 4 mL MPT posolyte were circulated into the channel (2 mm×2 mm×10 mm) from inlet by a peristaltic pump (Cole Parmer, 7528-20 with Masterflex 77390-00 PTFE pump head) in the continuous flow mode. The flow cell assembly process was conducted in an Ar-filled glove-box (Etelux, <1.0 ppm H_2O and <1.0 ppm O_2).

Electrochemical Characterizations: All the electrochemical characterizations were performed by using a VMP3 electrochemical testing unit (Bio-Logic). Galvanostatic charge/discharge tests of MPT posolytes were performed between 3.35 and 3.8 V versus Li^+/Li. Current density was calculated based on the carbon paper geometric surface area in the static cell (1 cm^2) and flow cell (0.1 cm^2). The specific capacity was calculated from the mass of active materials of MPT. The volumetric capacity was calculated from the total volume of posolyte. The energy density was calculated by integrating the discharge capacity and voltage normalized by the total volume of the posolyte. Electrochemical impedance spectroscopy (EIS) measurements used sinusoidal voltage oscillations of 20 mV amplitude at the open circuit voltage of the cells. The oscillation frequencies were swept from 100 kHz to 100 mHz with three repetitions for every test.

Material Characterizations: Scanning electron microscopy (SEM) characterization was performed on Quanta 400 FEI. The SEM samples for different cycle stages (Figure 4) were collected from cells disassembled at specified cycle stages in the glove-box. The residual solvent was evaporated before SEM observing. Fourier transform infrared spectroscopy (FTIR) was recorded with an ALPHA FTIR instrument (Bruker, Germany).

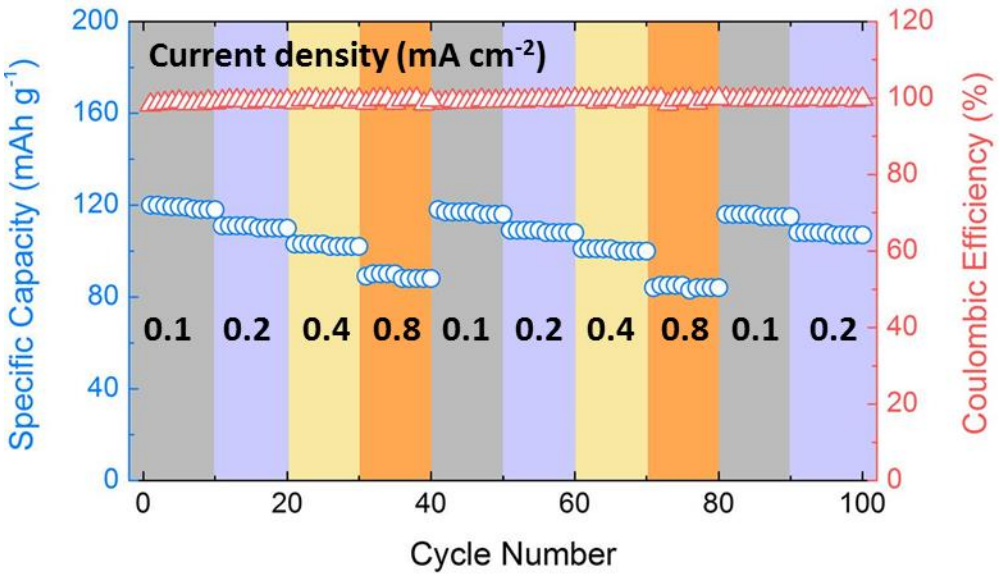

Figure S1. Rate capability tests of 50 mM MPT posolyte between 0.1 mA cm^{-2} to 0.8 mA cm^{-2} indicated in the text.

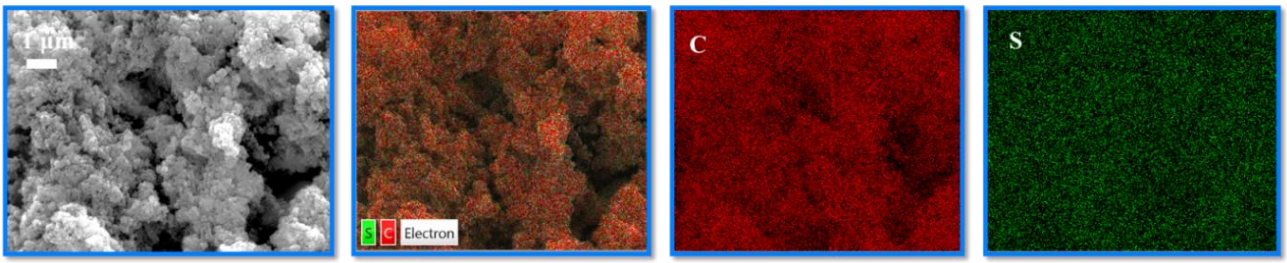

Figure S2. Energy-dispersive X-ray spectroscopy (EDX) images of the MPT-KB composite.

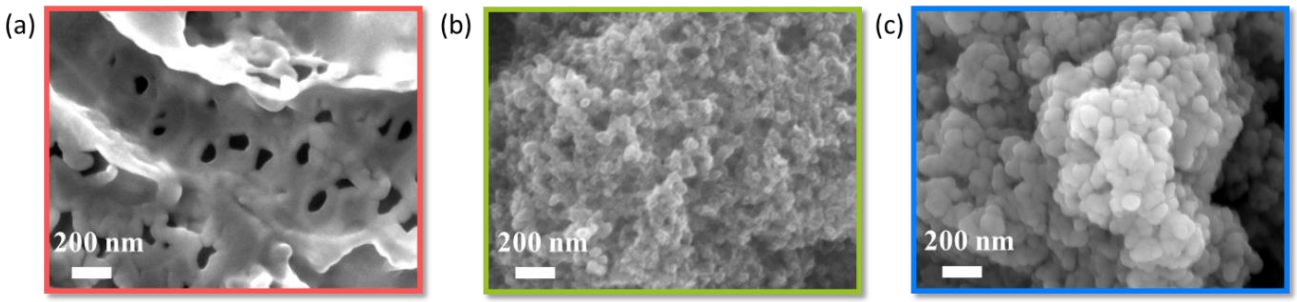

Figure S3. SEM images of (a) pristine MPT powder, (b) pristine KB and (c) 20MPT-5KB composite.

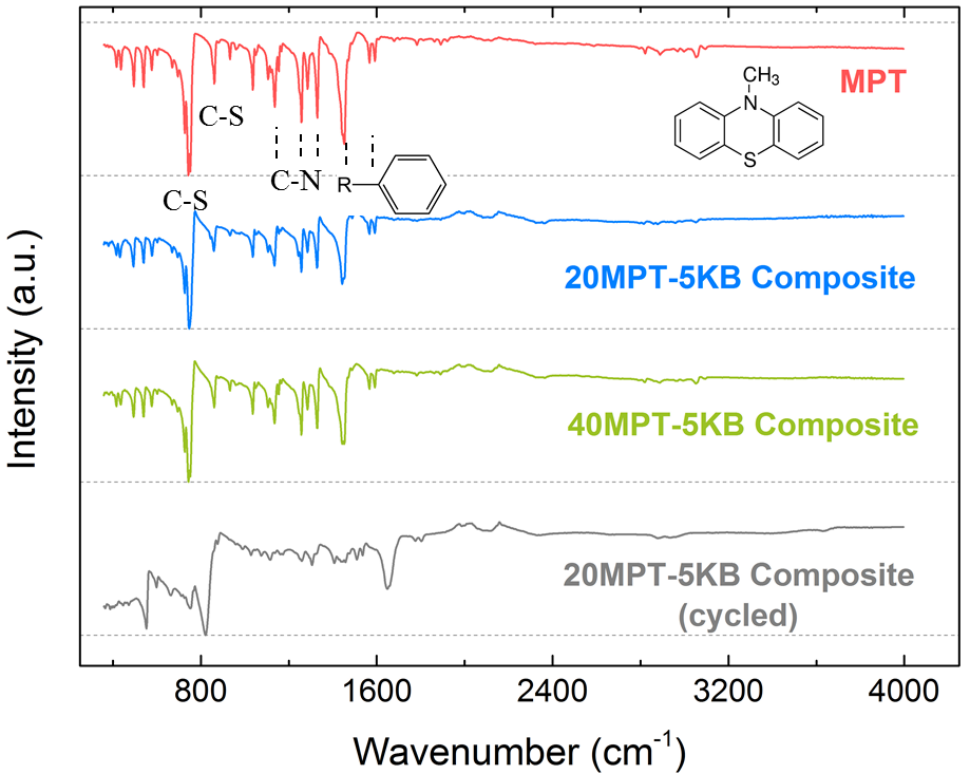

Figure S4. FTIR spectra of pristine MPT powder, 20MPT-KB and 40MPT-5KB composites and cycled 20MPT-5KB composite (40 cycles at 0.2 mA cm^{-2}). The peak assignments were referenced to Li et al. (*RSC Adv.*, 2015, 5, 71749). The absorption band at 1592, 1458 cm^{-1} is a typical peak of phenyl groups and the C–N vibration in MPT appears at 1133, 1259 and 1327 cm^{-1}. The peaks at 744 cm^{-1} and 862 cm^{-1} are assigned to the C–S vibration.

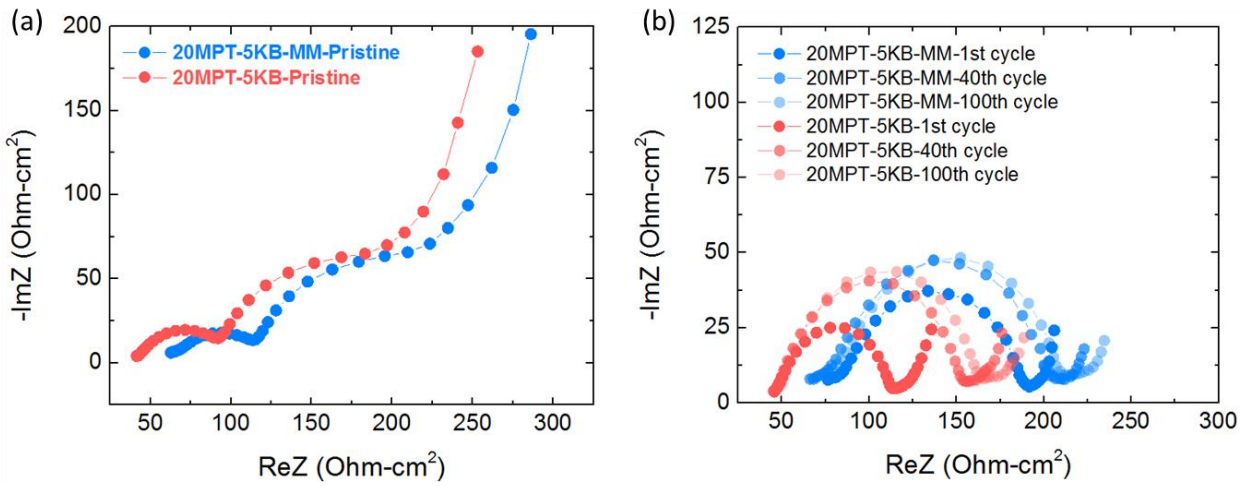

Figure S5. EIS comparison between 20MPT-5KB-MM and 20MPT-5KB posolytes at (a) pristine stage and (b) various cycling stages.

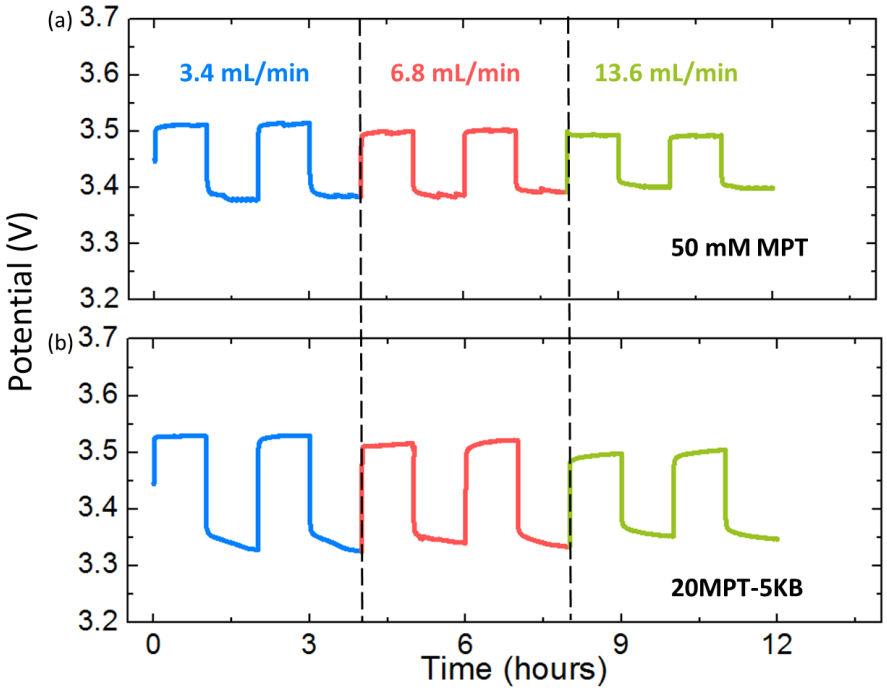

Figure S6. Continuous flow mode tests of LIONS flow battery: (a) The 50 mM MPT posolyte was used in a multiple step charge/discharge cycling tests at various flow rates. (b) The 20MPT-5KB posolyte was used in a multiple step charge/discharge cycling tests at various flow rates.

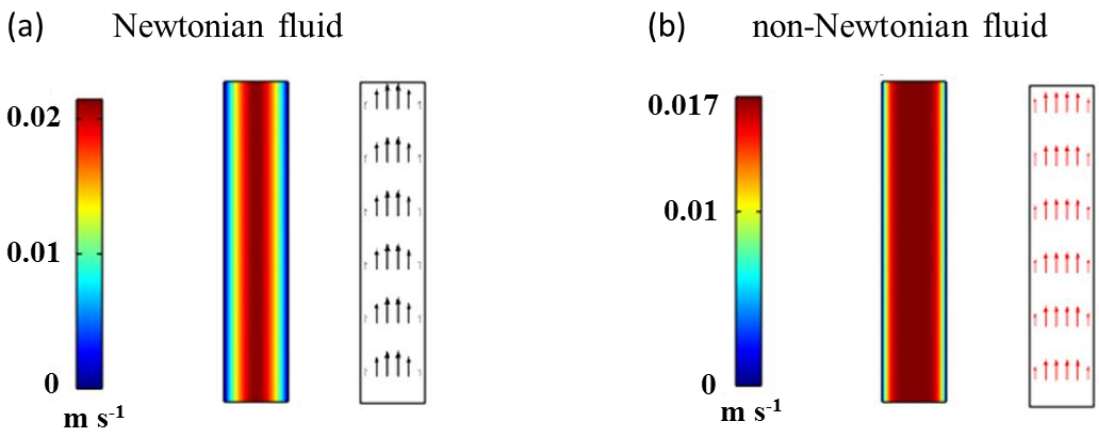

Figure S7. Flow field distribution of (a) Newtonian fluid and (b) non-Newtonian fluid.

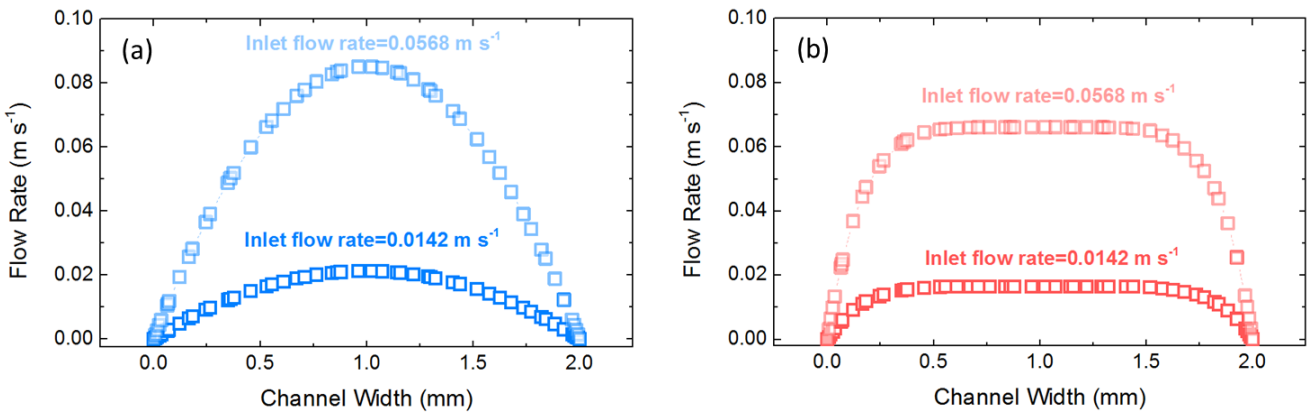

Figure S8. Inlet flow rate influence on the flow field distribution of (a) Newtonian fluid and (b) non-Newtonian fluid in the midplane of the channel.

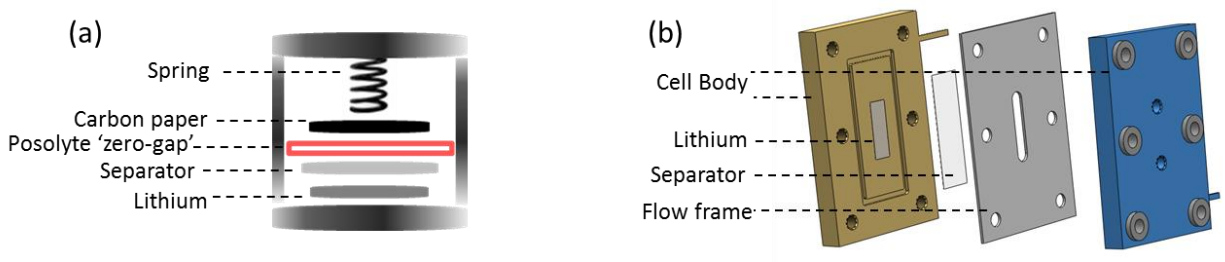

Figure S9. Schematic illustration and photographs of (a) static cell and (b) flow cell.

Table S1. Estimation of the chemical cost and rate performance of Li-based systems

Item / System	Active material price ($ kg^{-1})	Electrolyte price ($ kg^{-1})	Li metal price ($ kg^{-1})	Molecular Weight (kg mol^{-1})	Concentration (M)	Voltage vs Li/Li^{+} (V)	Electrolyte ratio (%)	Total cost ($ kWh^{-1})	Volumetric capacity (Ah L^{-1})	Energy density (Wh L^{-1})	Rate (mA cm^{-2})
Li-MPT suspension	10	5	50	0.213	2.23	3.5	55	43	55	190	0.8
Li-DMFc liquid	8	5	50	0.214	3	3.1	100	53	68	200	1.2
Li-TEMPO liquid	20	5	50	0.156	2	3.5	100	65	53	126	2.5
Li-MT/LT liquid	20 (MT) + 4 (LT)	5	50	0.186 (MT) + 0.287 (LT)	2 (MT) + 2 (LT)	3.6	100	83	54	200	1.0
Li-$LiFePO_4$ suspension	30	5	50	0.158	2.4	3.5	83	72	65	220	10
Li-S/LiI MRSSL	0.29 (S) + 50 (LiI)	5	50	0.032 (S) + 0.134 (LiI)	12.9 (S) + 2.7 (LiI)	2.2 (S) + 3.0 (LiI)	54	25	550	1100	10

All the prices are adopted from www.alibaba.com (Yang, Y.; Zheng, G.; Cui, Y., A membrane-free lithium/polysulfide semi-liquid battery for large-scale energy storage. *Energy Environ. Sci.* **2013,** 6, 1552-1558.) and the cost of electrolyte is based on ref. (Darling, R. M., Gallagher, K. G., Kowalski, J. A., Ha, S., & Brushett, F. R., Pathways to low-cost electrochemical energy storage: a comparison of aqueous and nonaqueous flow batteries. *Energy Environ. Sci.* **2014**, 7, 3459-3477.)

DMFc: 1,1-dimethylferrocene; TEMPO: 2,2,6,6-tetra-methylpiperidine-1-oxyl
MT: 4-methoxy-2,2,6,6-tetramethylpiperidine-1-oxyl; LT: lithium bis(trifluoromethanesulfonyl) imide

Note: We compare the cost analysis of Li-flow system using the posolyte indicated in the table. Lithium metal is also considered to provide the same amount of electron transfer of posolyte. Here is an example how the estimation is calculated (assuming that all the nonaqueous electrolytes' density is 1 g cm^{-3}).

$$((50\$\,kg^{-1} \times 0.007\,kg\,mol^{-1} + 10\,\$\,kg^{-1} \times 0.213\,kg\,mol^{-1}) \times 2.23\,M + 5\,\$\,kg^{-1} \times 1\,kg\,L^{-1} \times 55\%) \times \frac{1000}{3.5\,V \times 55\,Ah\,L^{-1}} = 43\,\$\,kWh^{-1}$$